Electromagnetic trace anomaly in a generalized linear sigma model

Amir H. Fariborz[1,*] and Renata Jora[2,†]

[1]*Department of Mathematics and Physics, SUNY Polytechnic Institute, Utica, New York 13502, USA*
[2]*National Institute of Physics and Nuclear Engineering, P.O. Box MG-6, Bucharest-Magurele, Romania*

We build the electromagnetic trace anomaly effective term for a generalized linear sigma model with two chiral nonets, one with a quark-antiquark structure and the other one with a four-quark content. In the leading order of this framework, we study the decays into two photons of the lowest isosinglet scalar mesons. We find that the direct inclusion of underlying mixing among two- and four-quark components in the trace anomaly term is essential in order for the model prediction to agree with the available experimental data on the decay width of $f_0(980)$ to two photons. Consequently, this sets a lower bound of 0.5 KeV on the decay with of $f_0(500)$ to two photons.

I. INTRODUCTION

The inverted mass spectrum of the low-lying scalar mesons with respect to the pseudoscalar and vector ones is a long-standing low-energy QCD puzzle [1] for which various solutions have been proposed [2–26], almost all of them dealing with the particular quark substructure of the scalar mesons. In a series of papers [27–32] we proposed and studied in detail a generalized linear sigma model with two chiral nonets, one with a two quark substructure and the other one with a four-quark content. In this framework the physical scalar states were found to have a significant admixture of two- and four-quark components, with those below 1 GeV generally containing a larger four-quark component compared to those above 1 GeV.

The generalized linear sigma model described in [27–32] contained, in addition to the relevant terms pertaining to mass and interactions, a term that mocks up the gluon axial anomaly. An extra term corresponding to the electromagnetic axial anomaly was further introduced in [30], where the decays of the pseudoscalar mesons to two photons were computed and studied with good agreement with experimental data. It seems then natural to extend this picture to include also the trace anomaly and analyze the decays of scalar mesons to two photons in the same context.

In Sec. II we briefly present our generalized linear sigma model followed by a derivation of the relevant term in the Lagrangian that leads to the correct electromagnetic trace anomaly in Sec. III. In Sec. IV we give our numerical computation for the decay of $f_0(500)$ and $f_0(980)$ to two photons and discuss the results.

II. GENERALIZED LINEAR SIGMA MODEL

The model of interest is a generalized linear sigma model with two chiral nonets, one with a quark-antiquark structure M and the other one with a four quark structure M',

$$M = S + i\Phi$$
$$M' = S' + i\Phi', \tag{1}$$

where S and S' represent the scalar nonets and Φ and Φ' the pseudoscalar nonets. The matrices M and M' transform in the same way under $SU(3)_L \times SU(3)_R$ but have different $U(1)_A$ transformation properties. The Lagrangian has the content

$$\mathcal{L} = -\frac{1}{2}\text{Tr}[D_\mu M D^\mu M^\dagger] - \frac{1}{2}\text{Tr}[D_\mu M' D^\mu M'^\dagger],$$
$$- V_0(M, M') - V_{SB}, \tag{2}$$

where

$$D_\mu M = \partial_\mu M - ieQMA_\mu + ieMQA_\mu$$
$$D^\mu M^\dagger = \partial^\mu M^\dagger + ieM^\dagger QA^\mu - ieQM^\dagger A^\mu \tag{3}$$

and $Q = \text{diag}(\frac{2}{3}, -\frac{1}{3}, -\frac{1}{3})$. Here in the leading order of the model, which corresponds to retaining only terms with no more than eight quark and antiquark lines,

$$V_0 = -c_2\text{Tr}[MM^\dagger] + c_4\text{Tr}[MM^\dagger MM^\dagger] + d_2\text{Tr}[M'M'^\dagger]$$
$$+ e_3(\epsilon_{abc}\epsilon^{def}M_d^a M_e^b M_f'^c + \text{H.c.})$$
$$+ c_3\left[\gamma_1\ln\left(\frac{\det M}{\det M^\dagger}\right) + (1-\gamma_1)\ln\left(\frac{\text{Tr}(MM'^\dagger)}{\text{Tr}(M'M'^\dagger)}\right)\right]^2. \tag{4}$$

The potential is invariant under $U(3)_L \times U(3)_R$ with the exception of the last term, which breaks $U(1)_A$. The symmetry breaking term has the form

*fariboa@sunyit.edu
†rjora@theory.nipne.ro

$$V_{SB} = -2\text{Tr}[AS], \tag{5}$$

where $A = \text{diag}(A_1, A_2, A_3)$ is a matrix proportional to the three light quark masses. The model allows for two-quark condensates $\alpha_a = \langle S_a^a \rangle$ as well as four-quark condensates $\beta_a = \langle S'^a{}_a \rangle$. Here we assume [33] isotopic spin symmetry, so $A_1 = A_2$ and

$$\alpha_1 = \alpha_2 \neq \alpha_3, \qquad \beta_1 = \beta_2 \neq \beta_3. \tag{6}$$

We also need the "minimum" conditions,

$$\left\langle \frac{\partial V_0}{\partial S} \right\rangle + \left\langle \frac{\partial V_{SB}}{\partial S} \right\rangle = 0, \qquad \left\langle \frac{\partial V_0}{\partial S'} \right\rangle = 0. \tag{7}$$

There are 12 parameters describing the Lagrangian and the vacuum. These include the six coupling constants given in Eq. (4), the two quark mass parameters ($A_1 = A_2, A_3$), and the four vacuum parameters ($\alpha_1 = \alpha_2, \alpha_3, \beta_1 = \beta_2, \beta_3$). The four minimum equations reduce the number of needed input parameters to eight. The details of numerical work for solving this system is given in [32], and for the readers convenience a summary is given in the Appendix.

The fields of interest are the neutral $I = 0$ scalar mesons,

$$f_a = \frac{S_1^1 + S_2^2}{\sqrt{2}}$$
$$f_b = S_3^3$$
$$f_c = \frac{S_1^{1\prime} + S_2^{2\prime}}{\sqrt{2}}$$
$$f_d = S_3^{3\prime}. \tag{8}$$

The scalars mix with each other within their group and form the physical states

$$\begin{pmatrix} f_1 \\ f_2 \\ f_3 \\ f_4 \end{pmatrix} = L_0^{-1} \begin{pmatrix} f_a \\ f_b \\ f_c \\ f_d \end{pmatrix}. \tag{9}$$

Here L_0 is the rotation matrix and depends on the model inputs. Based on the fit in Ref. [32], the first two physical states are

$$f_1 = f_0(500)$$
$$f_2 = f_0(980). \tag{10}$$

The experimental candidates for the remaining two states predicted by the model (f_3 and f_4) are $f_0(1370)$, $f_0(1500)$, and $f_0(1710)$. However, the exact identification requires inclusion of a scalar glueball which, for simplicity, was not included in the present order of the model. In this work our main focus is on $f_0(500)$ and $f_0(980)$.

III. THE TRACE ANOMALY TERM

The electromagnetic trace anomaly has the expression

$$\theta_\mu^\mu = \partial^\mu D_\mu = -\frac{\beta(e)}{2e} F^{\mu\nu} F_{\mu\nu}, \tag{11}$$

where θ_μ^μ is the trace of the energy momentum tensor, D_μ is the dilatation current, e is the electric charge, and $\beta(e)$ is the corresponding beta function. Equation (11) only displays the contribution to the trace anomaly due to electromagnetic group, which is relevant for the present work. Note that the full trace anomaly also contains contributions from the gluon fields and has the expression

$$\theta_\mu^\mu = \partial^\mu D_\mu = -\frac{\beta(e)}{2e} F^{\mu\nu} F_{\mu\nu} - \frac{\beta(g_3)}{2g_3} G^{a\mu\nu} G_{\mu\nu}^a, \tag{12}$$

where g_3 is the strong coupling constant and $G^{a\mu\nu}$ is the gluon tensor.

We apply the method introduced in [33–35] where for an arbitrary Lagrangian with fields η_A of mass dimension 1 and ξ_A with mass dimension 4,

$$\mathcal{L} = -\frac{1}{2} \sum_A \partial^\mu \eta_A \partial_\mu \eta_A - V(\eta_A, \xi_A), \tag{13}$$

the improved energy momentum tensor is defined as

$$\theta_{\mu\nu} = \delta_{\mu\nu} \mathcal{L} + \sum_A \partial_\mu \eta_A \partial_\nu \eta_A - \frac{1}{6} \sum_A (\partial_\mu \partial_\nu - \delta_{\mu\nu} \Box) \eta_A^2. \tag{14}$$

Here the fields η_A and ξ_A transform under the scale transformation,

$$\delta \eta_A = \eta_A + x_\mu \partial^\mu \eta_A$$
$$\delta \xi_A = 4\xi_A + x_\mu \partial^\mu \xi_A. \tag{15}$$

The trace of the energy momentum tensor can be written then as

$$\theta_\mu^\mu = \partial_\mu (x^\mu \mathcal{L}) - \delta \mathcal{L}, \tag{16}$$

which can be computed to be

$$\theta_\mu^\mu = \sum_A \left(4\xi_A \frac{\partial V}{\partial \xi_A} + \eta_A \frac{\partial V}{\partial \eta_A} \right) - 4V. \tag{17}$$

We shall use the expression in Eq. (17) to derive a suitable effective term that mocks up the electromagnetic anomaly.

Using this approach, it can be shown that the term

$$\mathcal{L}_s = bF^{\mu\nu}F_{\mu\nu}\left\{\tau_1\left[\ln\left(\frac{\det M}{\Lambda^3}\right) + \ln\left(\frac{\det M^\dagger}{\Lambda^3}\right)\right]\right.$$
$$\left. + \tau_2\left[\ln\left(\frac{\text{Tr}MM'^\dagger}{\Lambda^2}\right) + \ln\left(\frac{\text{Tr}M'M^\dagger}{\Lambda^2}\right)\right]\right\} \quad (18)$$

satisfies the anomaly in Eq. (11) provided that the dimensionless coefficients τ_1 and τ_2 satisfy the constraint $6\tau_1 + 4\tau_2 = 1$. Here in calculations the square of the electromagnetic tensor is assimilated to a scalar field of mass dimension 4. The term in Eq. (18) is chiral and $U(1)_A$ invariant, constructed by analogy with the axial anomaly and is minimal. It can, however, be expanded to include other possible contributions with higher orders of Λ (which is expected to be associated with Λ_{QCD}). By applying Eq. (17) and requiring that Eq. (11) is satisfied we determine $b = \frac{e^2}{12\pi^2}$, where we used $\beta(e) = \frac{1}{6\pi^2}e^3$.

In order to determine the coupling of the physical scalars, we expand the terms in the curly brackets in Eq. (18) around the vacuum expectation values of S and S' to show that these terms are equal to

$$\{\cdots\} = 2\tau_1\left[\frac{1}{\alpha_1}(S_1^1 + S_2^2) + \frac{1}{\alpha_3}S_3^3\right]$$
$$+ \frac{2\tau_2}{2\alpha_1\beta_1 + \alpha_3\beta_3}[\alpha_1(S_1^{1\prime} + S_2^{2\prime}) + \alpha_3 S_3^{3\prime}$$
$$+ \beta_1(S_1^1 + S_2^2) + \beta_3 S_3^3]. \quad (19)$$

Then the coupling of the physical states with the two photons can be read off easily as

$$F_{fi} = 4b\left[\tau_1\left(\frac{\sqrt{2}}{\alpha_1}(L_0)_{1i} + \frac{1}{\alpha_3}(L_0)_{2i}\right)\right.$$
$$+ \frac{\tau_2}{2\alpha_1\beta_1 + \alpha_3\beta_3}(\sqrt{2}\beta_1(L_0)_{1i} + \beta_3(L_0)_{2i}$$
$$\left. + \alpha_1\sqrt{2}(L_0)_{3i} + \alpha_3(L_0)_{4i}\right], \quad (20)$$

where $i = 1, \ldots, 4$ corresponds to the four isosinglet states (in this work only the first two are of interest). The amplitude of decaying to two photons are

$$A_i(f_i \to \gamma\gamma) = -F_{fi}(k_{1\mu}\epsilon_{1\nu} - k_{1\nu}\epsilon_{1\mu})$$
$$\times (k_{2\mu}\epsilon_{2\nu} - k_{2\nu}\epsilon_{2\mu}), \quad (21)$$

where k_1, k_2 are the photon momenta and ϵ_1, ϵ_2 are the photon polarizations. The decay width is given by

$$\Gamma(f_i \to \gamma\gamma) = F_i^2\frac{m_{f_i}^3}{16\pi}, \quad (22)$$

where m_{f_i} is the mass of the meson f_i.

IV. DECAY RATES AND DISCUSSION

As stated previously, our focus in this paper is on the two photon decays of $f_0(500)$ and $f_0(980)$. For $f_0(980)$ the experimental value of $\Gamma[f_0(980) \to \gamma\gamma] = 0.31^{+0.05}_{-0.04}$ KeV is listed in PDG [1]. Our model prediction for this decay width is found from Eqs. (20) and (22) with rotation matrices L_0 imported from prior work [32]. In this estimate the main model uncertainties stem from two of the experimental inputs ($m[\pi(1300)]$ and A_3/A_1) used in [32] to fix the model parameters. In addition, the two new parameters τ_1 and τ_2 in the trace anomaly in Eq. (18) are *a priori* unknown; therefore, after the constraint $6\tau_1 + 4\tau_2 = 1$ is considered, one of them still remains undetermined and needs to be varied [we choose to run τ_2 because it measures the direct effect of chiral nonet mixing on the anomaly term in (18)]. The result is shown in Fig. 1 versus τ_2 with the error bars representing the uncertainties due to variation of $m[\pi(1300)] = 1.2$–1.4 and $A_3/A_1 = 27$–30. The two horizontal lines give the experimental bounds [1] discussed above. It can be clearly seen that with small τ_2 (which measures the contribution of chiral mixing between nonets M and M') the model predictions do not overlap with the experimental values. This is very consistent with other observations within this model, where it is found that chiral mixing is essential for understanding the global properties of scalar mesons [32]. It is seen that for values of $\tau_2 \geq 0.7$ and $\tau_2 \leq -0.8$ the model predictions overlap with experiment.

Similarly, the prediction for the two-photon decay width of $f_0(500)$ is given in Fig. 2. Considering the acceptable ranges of $\tau_2 \geq 0.7$ and $\tau_2 \leq -0.8$, the prediction of this decay width shows the lower bound of approximately
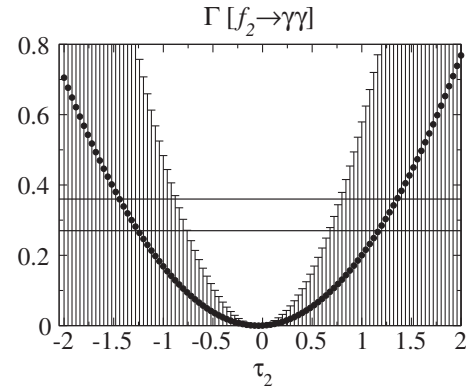

FIG. 1. Partial decay width to two photon (KeV) of f_2 [or $f_0(980)$] vs τ_2 predicted by the leading order of the generalized linear sigma model. The error bars represent the uncertainty of the model in its leading order and the circles represent the average predictions at each value of τ_2 (the uncertainties shown stem from the uncertainties of $m[\pi(1300)]$ in the range 1.2–1.4 and of the ratio A_3/A_1 varied in the range 27–30). The two parallel lines show the experimental range for this decay reported in PDG [1]. Overlap with experiment becomes possible for $\tau_2 \geq 0.7$ and $\tau_2 \leq -0.8$.
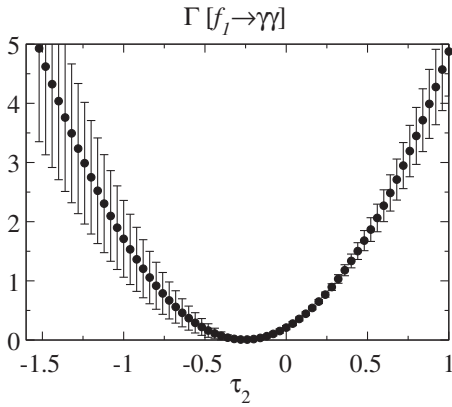
FIG. 2. Partial decay width to two photons (KeV) of f_1 [or $f_0(500)$] vs τ_2 predicted by the leading order of the generalized linear sigma model. The error bars represent the uncertainty of the model in its leading order and the circles represent the average predictions at each value of τ_2. The uncertainties shown stem from the uncertainties of $m[\pi(1300)]$ in the range 1.2–1.4 and of the ratio A_3/A_1 varied in the range 27–30. Comparing with Fig. 1, the acceptable region is $\tau_2 \geq 0.7$ and $\tau_2 \leq -0.8$, which sets a lower bound of approximately 0.5 KeV on the decay with of $f_0(500)$ to two photons.

0.5 KeV (occurring around $\tau_2 \approx -0.8$). This can be compared with other estimates in the literature such as 1.2 ± 0.04 KeV [37] or 10 ± 6 KeV [38]. In [39] the authors made a thorough amplitude analysis of the experimental data for $\gamma\gamma \rightarrow \pi^+\pi^-$ to find the position of the sigma pole at $0.441 - i0.272$ which corresponds to two scenarios for a decay width of $f_0(500)$ to two photons of 3.1 ± 0.5 KeV or 2.4 ± 0.4 KeV. More recently, performing a similar analysis, Dai and Pennington [40] found this decay width to be 2.05 ± 0.21 KeV. They also found $\Gamma[f_0(980)] \rightarrow \gamma\gamma = 0.32 \pm 0.05$ KeV. The decay widths of the low-lying scalar mesons were analyzed in the literature from the perspective that they proceed mainly through pion and kaon loops [41–44]. It is generally hypothesized, because of this assumption, that it is hard for these decays to be relevant for the quark substructure of the scalar mesons [1]. However, our results show that mixing among two- and four-quark components is essential for understanding the experimental data on decay width of $f_0(980)$ to two photons, hence, providing an indirect probe of the quark substructure of the light scalar mesons.

In summary, the lower bound of 0.5 KeV for the decay width of $f_0(500)$ to two photons obtained in this analysis (within the leading order of the generalized linear sigma model) is qualitatively consistent with other estimates [37–40]. A more precise prediction is expected when higher-order effects are taken into account. Within the current approach it was also shown that chiral nonet mixing is an essential ingredient in understanding this decay width, in which direct inclusion of mixing in modeling the trace anomaly is needed. This last point further supports the importance of the underlying mixing among two- and four-quark components in exploring the spectroscopy of light scalar mesons.

APPENDIX: BRIEF REVIEW OF THE NUMERICAL ANALYSIS FOR MODEL PARAMETERS AND ROTATION MATRICES

In this appendix we give a summary of the numerical determination of the eight independent Lagrangian parameters of Eqs. (2) and (4). Five of these eight are determined from the following masses together with the pion decay constant:

$$m[a_0(980)] = 980 \pm 20 \text{ MeV}$$
$$m[a_0(1450)] = 1474 \pm 19 \text{ MeV}$$
$$m[\pi(1300)] = 1300 \pm 100 \text{ MeV}$$
$$m_\pi = 137 \text{ MeV}$$
$$F_\pi = 131 \text{ MeV}. \tag{A1}$$

Since $m[\pi(1300)]$ has a large uncertainty (1.2–1.4 GeV), the Lagrangian parameters would depend on the choice of this experimental input. The sixth input is taken as the light "quark mass ratio" A_3/A_1, which are varied over its appropriate range (in this work we use the range 27–30).

The remaining two parameters (c_3 and γ_1) only affect the isosinglet pseudoscalars (whose properties also depend on the ten parameters discussed above). However, there are several choices for determination of these two parameters depending on how the four isosinglet pseudoscalars predicted in this model are matched to many experimental candidates below 2 GeV. The two lightest predicted by the model (η_1 and η_2) are identified with $\eta(547)$ and $\eta'(958)$ with masses

$$m^{\exp}[\eta(547)] = 547.853 \pm 0.024 \text{ MeV},$$
$$m^{\exp}[\eta'(958)] = 957.78 \pm 0.06 \text{ MeV}. \tag{A2}$$

For the two heavier ones (η_3 and η_4), there are six ways that they can be identified with the four experimental candidates above 1 GeV: $\eta(1295)$, $\eta(1405)$, $\eta(1475)$, and $\eta(1760)$ with masses

$$m^{\exp}[\eta(1295)] = 1294 \pm 4 \text{ MeV},$$
$$m^{\exp}[\eta(1405)] = 1409.8 \pm 2.4 \text{ MeV},$$
$$m^{\exp}[\eta(1475)] = 1476 \pm 4 \text{ MeV},$$
$$m^{\exp}[\eta(1760)] = 1756 \pm 9 \text{ MeV}. \tag{A3}$$

This leads to six scenarios considered in detail in [32]. The two experimental inputs for determination of the two parameters c_3 and γ_1 are taken to be $\text{Tr} M_\eta^2$ and $\det M_\eta^2$, i.e.,

TABLE I.   Rotation matrix L_0 for several values of A_3/A_1 and $m[\pi(1300)]$.

A_3/A_1	$m[\pi(1300)]$											
	1.2 (GeV)				1.3 (GeV)				1.4 (GeV)			
27.0	0.586	−0.110	0.800	0.065	−0.678	0.159	−0.717	−0.001	0.778	−0.233	−0.557	0.172
	0.204	0.192	−0.045	−0.959	−0.246	−0.284	0.169	0.911	0.240	0.467	0.376	0.764
	0.608	0.641	−0.380	0.275	−0.543	−0.629	0.374	−0.412	0.451	0.625	0.179	−0.612
	0.496	−0.735	−0.462	−0.020	−0.430	0.706	0.563	0.000	0.366	−0.580	0.719	−0.114
28.5	0.585	−0.105	0.801	0.065	−0.679	0.152	0.718	0.008	0.780	−0.223	−0.564	0.154
	0.198	0.185	−0.042	−0.962	−0.239	−0.274	−0.158	−0.918	0.232	0.449	0.359	0.785
	0.609	0.643	−0.382	0.266	−0.544	−0.632	−0.384	0.396	0.450	0.634	0.210	−0.592
	0.498	−0.736	−0.459	−0.019	−0.432	0.708	−0.558	−0.003	0.366	−0.589	0.714	−0.098
30.0	0.585	−0.101	0.802	0.065	0.680	−0.146	0.718	0.014	0.782	−0.214	−0.569	0.138
	0.192	0.179	−0.040	−0.964	0.232	0.264	−0.148	−0.924	0.225	0.431	0.343	0.804
	0.610	0.644	−0.384	0.257	0.544	0.635	−0.393	0.381	0.450	0.642	0.239	−0.572
	0.499	−0.737	−0.456	−0.018	0.433	−0.711	−0.554	−0.006	0.367	−0.597	0.708	−0.085

$$\text{Tr}(M_\eta^2) = \text{Tr}(M_\eta^2)_{\text{exp}},$$
$$\det(M_\eta^2) = \det(M_\eta^2)_{\text{exp}}. \qquad (A4)$$

Moreover, for each of the six scenarios, γ_1 is found from a quadratic equation, and as a result, there are all together 12 possibilities for determination of γ_1 and c_3. Since only Tr and det of experimental masses are imposed for each of these 12 possibilities, the resulting γ_1 and c_3 do not necessarily recover the exact individual experimental masses; therefore, the best overall agreement between the predicted masses (for each of the 12 possibilities) were examined in [32]. Quantitatively, the goodness of each solution was measured by the smallness of the following quantity:

$$\chi_{sl} = \sum_{k=1}^{4} \frac{|m_{sl}^{\text{theo}}(\eta_k) - m_s^{\text{exp}}(\eta_k)|}{m_s^{\text{exp}}(\eta_k)}, \qquad (A5)$$

in which s corresponds to the scenario (i.e., $s = 1, …, 6$) and l corresponds to the solution number (i.e., $l = $ I, II).

The quantity $\chi_{sl} \times 100$ gives the overall percent discrepancy between our theoretical prediction and experiment. For the six scenarios and the two solutions for each scenario, χ_{sl} was analyzed in Ref. [32]. For the third scenario [corresponding to identification of η_3 and η_4 with experimental candidates $\eta(1295)$ and $\eta(1760)$] and solution I the best agreement with the mass spectrum of the eta system was obtained (i.e., χ_{3I} was the smallest). Furthermore, all six scenarios were examined in the analysis of $\eta' \to \eta\pi\pi$ decay in [45] and it was found that the best overall result (both for the partial decay width of $\eta' \to \eta\pi\pi$ as well as the energy dependence of its squared decay amplitude) is obtained for scenario 3I, consistent with the analysis of Ref. [32]. In this work, we use the result of the 3I scenario.

The numerical values for the rotation matrix L_0 defined in (20) can be consequently determined. Since two of the model inputs A_3/A_1 and $m[\pi(1300)]$ have large uncertainties, the numerical values of these rotation matrices naturally have some dependencies on these two inputs. Table I gives numerical values of L_0 for three values of $m[\pi(1300)]$ and three values of A_3/A_1.

[1] C. Patrignani *et al.* (Particle Data Group Collaboration), Chin. Phys. C **40**, 100001 (2016).

[2] E. van Beveren, T. A. Rijken, K. Metzger, C. Dullemond, G. Rupp, and J. E. Ribeiro, Z. Phys. C **30**, 615 (1986).

[3] D. Morgan and M. Pennington, Phys. Rev. D **48**, 1185 (1993).

[4] A. A. Bolokhov, A. N. Manashov, M. V. Polyakov, and V. V. Vereshagin, Phys. Rev. D **48**, 3090 (1993).

[5] N. N. Achasov and G. N. Shestakov, Phys. Rev. D **49**, 5779 (1994); N. N. Achasov, arXiv:0810.2601.

[6] R. Kamiński, L. Leśniak, and J. P. Maillet, Phys. Rev. D **50**, 3145 (1994).

[7] F. Sannino and J. Schechter, Phys. Rev. D **52**, 96 (1995).

[8] G. Janssen, B. C. Pearce, K. Holinde, and J. Speth, Phys. Rev. D **52**, 2690 (1995).

[9] R. Delbourgo and M. D. Scadron, Mod. Phys. Lett. A **10**, 251 (1995).

[10] N. A. Törnqvist and M. Roos, Phys. Rev. Lett. **76**, 1575 (1996).

[11] M. Svec, Phys. Rev. D **53**, 2343 (1996).

[12] S. Ishida, M. Y. Ishida, H. Takahashi, T. Ishida, K. Takamatsu, and T Tsuru, Prog. Theor. Phys. **95**, 745 (1996).

[13] M. Harada, F. Sannino, and J. Schechter, Phys. Rev. D **54**, 1991 (1996).

[14] A. V. Anisovich and A. V. Sarantsev, Phys. Lett. B **413**, 137 (1997).

[15] D. Black, A. H. Fariborz, F. Sannino, and J. Schechter, Phys. Rev. D **58**, 054012 (1998).

[16] J. A. Oller, E. Oset, and J. R. Pelaez, Phys. Rev. Lett. **80**, 3452 (1998).

[17] V. Elias, A. H. Fariborz, F. Shi, and T. G. Steele, Nucl. Phys. **A633**, 279 (1998).

[18] K. Igi and K. Hikasa, Phys. Rev. D **59**, 034005 (1999).

[19] D. Black, A. H. Fariborz, F. Sannino, and J. Schechter, Phys. Rev. D **59**, 074026 (1999).

[20] D. Black, A. H. Fariborz, S. Moussa, S. Nasri, and J. Schechter, Phys. Rev. D **64**, 014031 (2001).

[21] R. L. Jaffe, Phys. Rev. D **15**, 267 (1977).

[22] J. D. Weinstein and N. Isgur, Phys. Rev. Lett. **48**, 659 (1982).

[23] D. Black, A. H. Fariborz, and J. Schechter, Phys. Rev. D **61**, 074001 (2000).

[24] T. Teshima, I. Kitamura, and N. Morisita, J. Phys. G **28**, 1391 (2002); **30**, 663 (2004); F. Close and N. Tornqvist, *ibid.* **28**, R249 (2002); A. H. Fariborz, Int. J. Mod. Phys. A **19**, 2095 (2004); **19**, 5417 (2004); **74**, 054030 (2006).

[25] M. Napsuciale and S. Rodriguez, Phys. Rev. D **70**, 094043 (2004); F. Giacosa, Th. Gutsche, V. E. Lyubovitskij, and A. Faessler, Phys. Lett. B **622**, 277 (2005); J. Vijande, A. Valcarce, F. Fernandez, and B. Silvestre-Brac, Phys. Rev. D **72**, 034025 (2005); S. Narison, Phys. Rev. D **73**, 114024 (2006); L. Maiani, F. Piccinini, A. D. Polosa, and V. Riquer, arXiv:hep-ph/0604018; J. R. Pelaez, Phys. Rev. Lett. **92**, 102001 (2004); J. R. Pelaez and G. Rios, Phys. Rev. Lett. **97**, 242002 (2006); F. Giacosa, Phys. Rev. D **75**, 054007 (2007).

[26] G. 't Hooft, G. Isidori, L. Maiani, A. D. Polosa, and V. Riquer, Phys. Lett. B **662**, 424 (2008).

[27] A. H. Fariborz, R. Jora, and J. Schechter, Phys. Rev. D **72**, 034001 (2005).

[28] A. H. Fariborz, R. Jora, and J. Schechter, Phys. Rev. D **77**, 034006 (2008).

[29] A. H. Fariborz, R. Jora, and J. Schechter, Phys. Rev. D **76**, 114001 (2007).

[30] A. H. Fariborz and R. Jora, Phys. Rev. D **95**, 114001 (2017).

[31] A. H. Fariborz, R. Jora, and J. Schechter, Phys. Rev. D **77**, 094004 (2008).

[32] A. H. Fariborz, R. Jora, and J. Schechter, Phys. Rev. D **79**, 074014 (2009).

[33] J. Schechter and Y. Ueda, Phys. Rev. D **3**, 2874 (1971).

[34] C. Rosenzweig, J. Schechter, and C. G. Trahern, Phys. Rev. D **21**, 3388 (1980).

[35] C. Rosenzweig, A. Salomone, and J. Schechter, Phys. Rev. D **24**, 2545 (1981).

[36] D. Black, A. H. Fariborz, S. Moussa, S. Nasri, and J. Schechter, Phys. Rev. D **64**, 014031 (2001).

[37] J. Bernabeu and J. Prades, Phys. Rev. Lett. **100**, 241804 (2008).

[38] A. Courau *et al.*, Nucl. Phys. **B271**, 1 (1986).

[39] M. R. Pennington, T. Mori, S. Uehara, and Y. Watanabe, Eur. Phys. J. C **56**, 1 (2008).

[40] L.-Y. Dai and M. R. Pennington, Phys. Rev. D **90**, 036004 (2014).

[41] N. N. Achasov and G. N. Shestakov, Z. Phys. C **41**, 309 (1988); Phys. Rev. D **72**, 013006 (2005); **77**, 074020 (2008).

[42] F. Giacosa, Th. Gutsche, and V. E. Lyubovitskij, Phys. Rev. D **77**, 034007 (2008).

[43] J. A. Oller, L. Roca, and C. Schat, Phys. Lett. B **659**, 201 (2008).

[44] Yu. L. Kalinovsky and M. K. Volkov, Phys. At. Nucl. **73**, 443 (2010).

[45] A. H. Fariborz, J. Schechter, S. Zarepour, and M. Zebarjad, Phys. Rev. D **90**, 033009 (2014).